This full text paper was peer reviewed at the direction of IEEE Communications Society subject matter experts for publication in the IEEE ICC 2010 proceedings

Field Trial Results of a 4x4 MIMO-OFDM Real Time Testbed

Omar A. Nasr*, Oscar Y. Takeshita+, Weijun Zhu+ and Babak Daneshrad*
* Wireless Integrated Research Lab, EE department, UCLA +SilvusTechnologies Inc., Los Angeles, CA, 90024

***Abstract*—the results of a field trials campaign in a park, a wide street, a narrow street and office environments are presented in this paper. The trials are carried out using a real time 4x4 MIMO-OFDM testbed working in the 2.4 GHz ISM band and a 20 MHz bandwidth. The testbed supports both spatial multiplexing and transmit and receive diversity. We compare the system performance using different number of spatial streams in different environments. We also determine the maximum number of spatial streams that can be supported in the indoor and outdoor environments respectively. We found that the maximum achievable throughput for the system in the indoor environment is almost double the maximum achievable throughput in the outdoor environment at the same receive power. This is mainly due to the richness of scattering elements in an indoor setting. Our outdoor trials showed that supporting more than two spatial streams will not introduce any throughput gain.**

Keywords-testbed; field trials; MIMO-OFDM; channel condition number

I. INTRODUCTION

Theoretical studies and simulations have shown a significant increase in the capacity of wireless channels by using multiple antennas technology [1].A diversity gain can also be achieved by adding multiple antennas at transmit and receive side[1]. Motivated by these studies, MIMO-OFDM technology has recently been adopted by several wireless standards such as WiFi, WiMax, and 3G-LTE among others. To validate these theoretical results, several testbeds have been built. The first category of testbeds focuses on MIMO channel sounding and capacity measurements in real environments (e.g [7]-[8]). Another category of testbeds focuses on the capacity of MIMO-OFDM systems (e.g [5]). The third category are focused on the practicality of implementing real-time MIMO platforms, (e.g [3]-[4]), and do not look to validate/dis-prove the theoretical work.

In[6], some indoors field measurements were carried out but no analysis of the results were presented. In [3], a non-real-time testbed was used to carry out field trials at only three locations in an office environment and made some analysis for the results. The testbeds reported in [10]-[11] are real time testbeds, but they do not provide data analysis of the results.

One of the major challenges in translating theoretical gains to practical system performance is the proper characterization of all impairments consisting of RF, and algorithmic non-idealities (i.e. finite precision, estimation error, etc.). This is a formidable task. Our approach to address this is to build a real-time testbed and characterize its performance under controlled and uncontrolled environments. By repeating the experiments over an ever increasing set of environments trends can be observed that would lead to adjustments in the theoretical predictions. Within the scope of this conference paper, our aim is to introduce the community to the capabilities, and share the first of many field trial results using the testbed.

In this paper, A real time MIMO-OFDM 4x4 testbed was developed and used to evaluate the system performance in real indoor and outdoor environments. A comparison between the performances using different number of spatial streams in different fields is presented. We also determine the maximum number of spatial streams that can be supported in different environments using our testbed. Our trials involving communications between two cars in an outdoor environment shows that supporting more than two spatial streams will not introduce any throughput gain. The same testbed used in an indoor office environment was able to support 3 to 4 spatial streams, due to the richness of spatially varied paths between the two ends of the link.

The paper is organized as follows: in section II, the different parts of the testbed are described, including the baseband algorithms, the RF components and the board used to host the hardware. Section III discusses the RF calibration and the testbed calibration over the cable. In Section IV we describe the field trial environment. Section V presents and discusses the field measurement results with emphasis on comparing the performance of different number of spatial streams in different fields. The conclusions are presented in section section VI.

II. SYSTEM DESCRIPTION

A. Baseband

The baseband portion of the testbed is an upgrade to that used in [14] The transmitted packet structure is the same as the packet structure in [2] The transmit packet parameters are listed in table 1. A block diagram of the receiver is shown in Fig. 1. The first block is the AGC, which uses an algorithm similar to [13].The AGC measures the energies of N samples of the incoming signal on the four receive antennas and compares them to a threshold that is 4dB above the noise level

978-1-4244-6404-3/10/$26.00 ©2010 IEEE

of the boards. When the received signal in any one of the four antennas is above the threshold, the AGC adjusts the LNA and VGA settings depending on the receive signal strength. It also triggers the packet detection block, which uses an autocorrelation based approach [10] to look for the periodicity embedded into the packet preamble. A fine search for the OFDM block boundary is carried out by performing the autocorrelation with different lags and choosing the lag that leads to the maximum correlation value as the packet start. The frequency offset between the Tx and the Rx is estimated by dividing the phase of the maximum autocorrelation by the lag leading to the maximum autocorrelation. A fine estimation of the frequency offset is performed by calculating the phase of the autocorrelation between two identical halves of the LLTF field of the preamble [2]. This is explained in details in [10]. The two halves of the LLTF are then averaged, transferred to the frequency domain and the "legacy" channel estimates for all subcarriers are calculated in the frequency domain [2]. The estimated channels along with the noise estimates are used to determine the packet parameters (modulation and coding schemes used, packet length, .. etc). The last part of the preamble is the HT-LTF [2] which is used to calculate the MIMO channel estimates between each spatial stream and receive antenna. The implementation of the MIMO MMSE decoder is described in detail in [9]. It is a "matrix inversion free" MIMO MMSE detector that uses dynamic scaling to reduce the hardware complexity of the MIMO decoder. After the MIMO decoder, the decoded symbols are QAM demapped, de-interleaved, depunctured and passed through a soft decision FEC Viterbi decoder .

The baseband design runs on a custom board consisting of two Xilinx Virtex 5 XC5VLX220-1FFG1760C's and a Power PC that acts as the central controller for the board.

B. RF boards

Four RF boards at both the Tx and the Rx are connected to the digital output from the PHY FPGA. The basic chip on the boards is the Maxim MAX2829, which is a dual band (2.4GHz or 5GHz) RF IC. A 12-bit ADC/DAC (AD9863) is used to convert between analog and digital. A 30 dB fixed gain power amplifier (FMPA2151) is added in the TX signal path which provides a variable output power between -7dBm and 17dBm.

TABLE 1: Transmit packet parameters

Parameter	Value
Signal bandwidth	20 MHz
FFT size	64
Subcarrier frequency spacing	312.5 kHz
FFT period	3.2 us
Guard interval	800 ns
Number of data subcarriers	52
Number of pilot subcarriers	4

III. SYSTEM CALIBRATION

The first step in system calibration is the determination of the RF impairments of the boards. The average values of the impairments, as measured with general purpose laboratory instruments are shown in Table 2 .

In order to characterize the performance loss due to the fixed point implementation on the FPGA, a bit-accurate MATLAB simulation of the VHDL implementation on the FPGA was used. The performance of the floating point and the fixed point MATLAB simulations in case of AWGN is shown in Fig. 2. There is a very small performance loss due to the fixed point implementation (less than 0.3 dB).

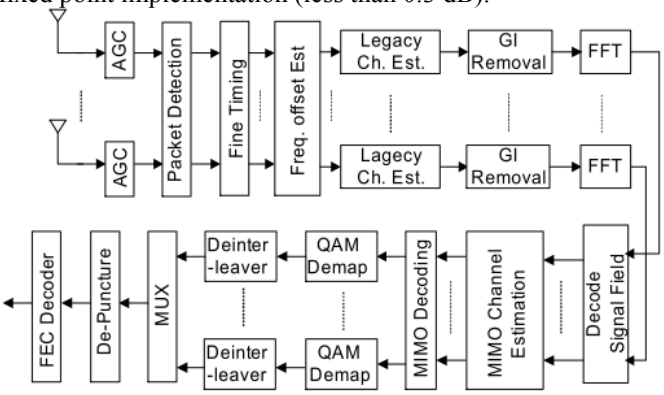

Fig. 1 . Block diagram of the receiver

TABLE 2
Average value of the RF impairments of the boards

RF imperfection	Median value of the four boards
I/Q imbalance [image rejection]	43dBs
Phase noise @ 1MHz	-100dBc
Freq offset between Tx/Rx	9kHz
Tx LO leakage	-17 dBm
Average Noise level	-81 dBm

To characterize the effect of the RF impairments on the system performance, we connected each pair of Tx and Rx ports with a cable and a variable attenuator. A fixed Tx power of 10 dBm was transmitted from all four Tx boards and four variable attenuators were used to change the Rx SNR between 5 dB and 30 dB. Before sending the data, we measured the noise powers for the four boards while connecting the attenuators and the cables between the Tx and the Rx. During the packets transmission, the AGC measures the power of the received packets at the four boards and reports the values of the Rx powers to the host. The SNRs at the four boards were not equal because of the accuracy of the attenuators and component mismatches. For fair comparison, we replicated these differences in the floating point simulation. The maximum variation between the SNRs of the individual branches was about 1 dB. Fig. 3 shows the results of using modes 1, 4 and 6 (table 3) with four spatial streams and thousand byte/packets. The results are plotted for both over the cable testing and floating point simulations. For modes 1 and 4, the system has 1dB loss up to PER = 10^{-2}, while for mode 6, the system has a loss of 3 dB at PER = 10^{-2}.

IV. MODES AND FIELDS DESCRIPTION

A. Modes tested

In all field trials, we send 1000 byte/packets with the modes in table 3. The total Tx power from all antennas is fixed to be 50 mW (17 dBm). We test sending packets using one or two spatial streams over the four Tx antennas using Cyclic Delay Diversity (CDD). Three spatial stream transmission is also tested but the data is transmitted using three antennas while

keeping the same total Tx power (50 mW). Four spatial stream transmission is tested using direct mapping to the four Tx antennas. When multiple spatial streams are transmitted, the data is sent from each stream using the same modulation and coding. In all cases, four receive antennas are used. The maximum throughput that can be supported is 256 Mbps when we send mode 7 with four spatial streams. This corresponds to 15.75 bps/Hz when we consider the data bandwidth of 16.25 MHz (the remainder of the 20 MHz bandwidth is used to send pilot subcarriers or guard subcarriers).

TABLE 3
Modulation and Coding for different modes

Mode	Code rate	Modulation	Bit rate per stream
0	½	BPSK	6.5 Mbps
1	½	QPSK	13 Mbps
2	¾	QPSK	19.5 Mbps
3	½	16QAM	26 Mbps
4	¾	16QAM	39 Mbps
5	2/3	64QAM	52 Mbps
6	¾	64QAM	58.5 Mbps
7	5/6	64QAM	65 Mbps

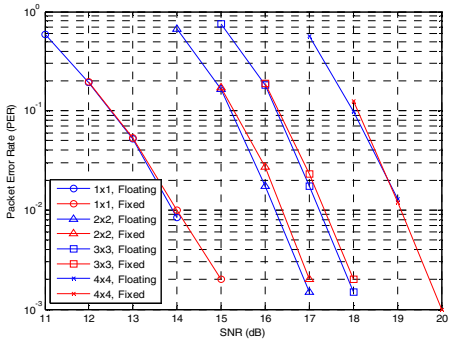

Fig. 2. Fixed and floating point simulations

B. Fields description:

1) Outdoor environments:

Three different outdoors environments were tested. In all these tests, the TX was on top of a small car (1.5 m height) and the spacing between antennas was 1 wavelength (Fig. 4). The Rx antennas were stuck on top of a van (2.2 m height) and the antenna spacing was 2 wavelengths, as shown in Fig. 5. For all outdoor trials, we used the tall HG2409RD-SM antennas at the Tx. For both indoor and outdoor environments, HyperGain RE05U antennas were used at the receiver. The first environment is a park (Fig. 6). The Tx was in the parking lot of the park while the Rx moved in the parking lot and then around the park. Only few cars were moving in that route. Few cars were parking but the Rx van was higher than most of them. The tree density in the park is intense on the edges and light inside the park itself where it is mostly green grass. We also tested a wide street (40m wide), where the transmitter was located at the intersection between the wide street and another narrow street. The receiver moved in the wide street with few cars that are lower than the van used to host the receiver. A narrow street (17m width) was our final outdoor environment, where the transmitter was located at the intersection between two narrow streets and the receiver moved in one of them. There were cars parking on the sides of the street during the trial time.

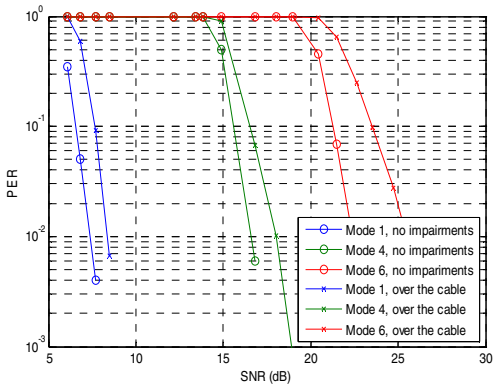

Fig. 3. Effect of RF impairments on system performance

2) Indoor environment:

The indoor field trials were carried out within a modern high-rise building with concrete construction. The office floor plan is shown in Fig. 7. The receiver moved to 65 different locations in the field. The Tx was on a table and the Rx moved on a small metal cart. The Tx antenna spacing was one wavelength. The Rx antennas were distributed around the Rx cart, and the spacing between different antennas was between 2-3 wavelengths.

V. Data Analysis for Field Trials

A. Performance metrics

The performance metric used to analyze the data collected from the fields is based on the effective throughput for each mode and number of spatial streams. The effective throughout is defines as $R_{i,N_{ss}}^{eff} = R_i.N_{ss}.(1-PER_{i,N_{ss}})$, where R_i is the PHY throughout of mode i, N_{ss} is the number of spatial stream and $PER_{i,N_{ss}}$ is the packet error rate when the data is transmitted using mode i and N_{ss} spatial streams. For every point at each environment and for each spatial stream, the effective throughputs of different modes are compared and the highest throughput is selected as the Best Achievable Throughput (BAT).

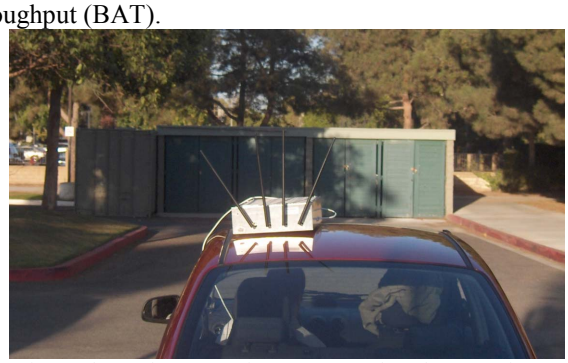

Fig. 4. The outdoor transmitter: MWLAN board on top of a car

Fig. 5. The outdoor receiver: tall antennas on top of a van

Fig. 6. Satellite picture of an outdoor environment (park)

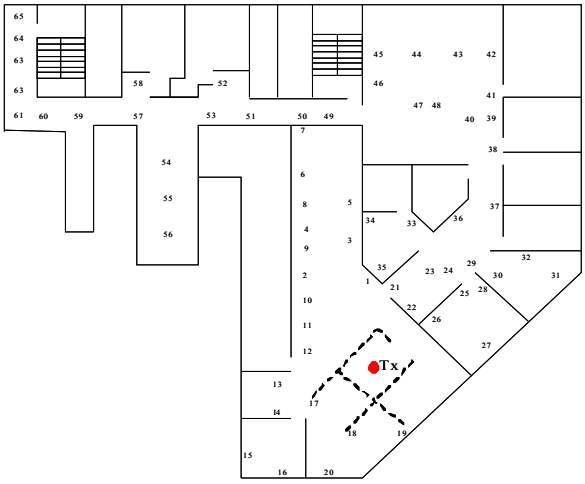

Fig. 7. Floor plan of the office and the locations of the Tx and Rx

B. Field measurement results and comparison

The indoor environment is ideal for MIMO communications because of the existence of a scatter rich environment. Fig. 8 shows the performance of different number of spatial streams and the corresponding Rx powers at different points. We have renumbered the points to have the lowest received power points first. It is clear that using three spatial streams is better than using any other number of spatial streams, implying that the indoor channel had three strong Eigen-modes. Moreover, we see a doubling of throughput when going from one to two spatial streams; however, going from 2 to 3 spatial streams only delivers an average throughput improvement of 25% as compared to the 50%, which is the theoretical gain. This result suggests that at least 50% and possibly 75% of the channels encountered had a strong third eigenmode.

In indoors settings, the maximum distance between the transmitter and the receiver is 30m.

Fig. 9 shows the BAT for different number of spatial streams and the received powers at different points in the outdoor environments. The underlying trend points to the inability of the system to reliably support more than a single spatial stream. We see that when the Rx power is high, the system can support two, and possibly three spatial streams, however, due to the weakness of the Eigen modes associated with the second and third spatial streams as soon as the SNR drops, the performance of these systems degrades and the one spatial stream system dominates. This trend becomes more and more pronounced as we go from the park to the wide street and ultimately to the narrow street, and is directly correlated with the angular spread of the waveforms incident at the receiver. The trend can also be seen by looking at Table 4 which summarizes the average reciprocal condition number (RCN) for the 2nd, 3rd, and 4th Eigen modes of the channel. We see that the indoor channel has three strong Eigen modes with RCNs greater than 0.3. On the other hand the outdoor channels have only one strong Eigen mode, the RCN for the second Eigen mode is less than 0.3 and drops as we go from the Park to the wide street and ultimately to the narrow street.

The average performance at different points in the two fields is shown in Fig. 10. At Rx signal strength = -55 dBm, the BAT of the indoor environment is 165 Mbps while it is about 93 Mbps for the Park environment.

The results suggest that an RCN of 0.3 could be used as a soft delimiter between deciding whether or not the particular Eigen mode is strong enough to support data communications.

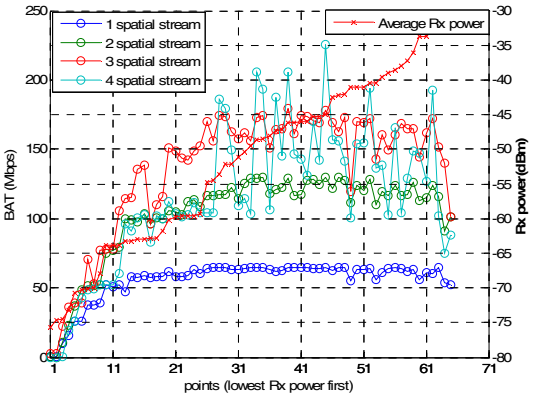

Fig. 8. Indoor *BAT* and average Rx power

TABLE 4: Reciprocal condition number in the two fields

Trial	*RCN4*	*RCN3*	*RCN2*	Max dist (m)
Indoor	0.1053	0.3201	0.5511	30
Park	0.0481	0.1427	0.2833	260
Wide street	0.0426	0.1222	0.2539	420
Narrow street	0.0350	0.1137	0.2483	280

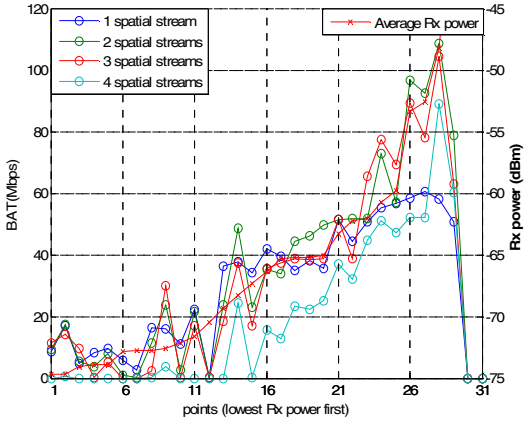

(a) Park

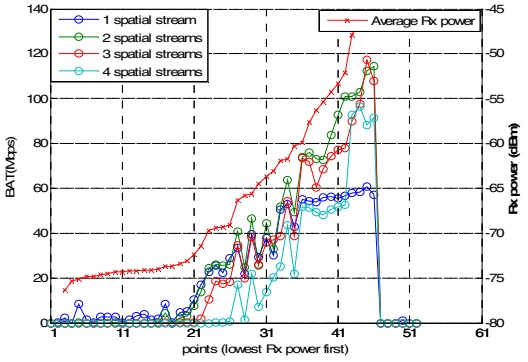

(b)Wide street

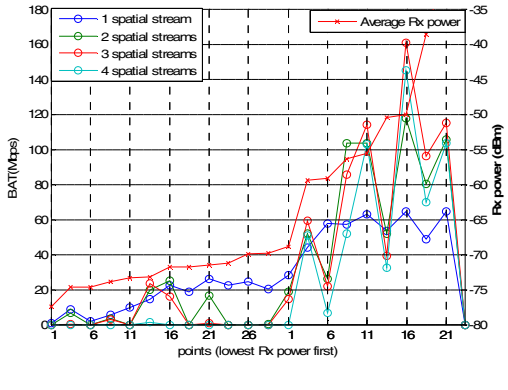

(c)Narrow street

Fig. 9. Comparison between different spatial streams in outdoor environments

VI. Conclusion

In this paper, the results of a field trial campaign using a real-time 4x4 MIMO-OFDM testbed were presented. An office environment and several outdoor environments were selected for the campaign. The results are a first among a series of contributions that quantify the performance of end to end MIMO systems as a function of antenna configuration, polarization, processing and the environment.

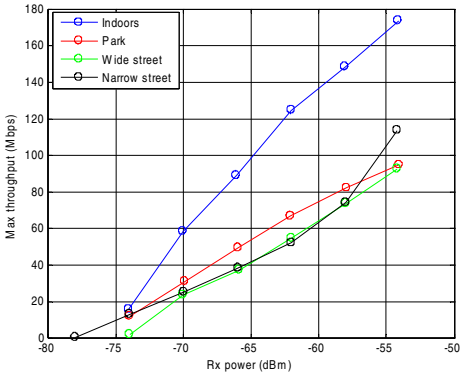

Fig. 10. Comparison between BAT in the indoor and outdoor fields

References

[1] David Tse , Pramod Viswanath, Fundamentals of wireless communication, Cambridge University Press, New York, NY, 2005.

[2] IEEE P802.11n/D2.00, Feb. 2007.

[3] Weidong Xiang, Paul Richardson, Brett Walkenhorst, Xudong Wang, and Thomas Pratt, "A High-Speed Four-Transmitter Four-Receiver MIMO OFDM Testbed: Experimental Results and Analyses," *EURASIP Journal on Applied Signal Processing,* vol. 2006, Article ID 45401, 10 pages, 2006.

[4] J. Rinas, R. Seeger, L. Brötje, S. Vogeler, T. Haase, and K.-D. Kammeyer, "A Multiple-Antenna System for ISM-Band Transmission," EURASIP Journal on Applied Signal Processing, vol. 2004, no. 9, pp. 1407-1419, 2004.

[5] S. Lang and B. Daneshrad, "From architecture to implementation of a wireless, multiple antenna testbed," *IEEE International Symposium on Circuits and Systems, 2005. ISCAS 2005,* vol. 5, pp. 4465-4468 Vol. 5, 23-26 May 2005.

[6] S. Nanda, R. Walton, J. Ketchum, M. Wallace and S. Howard, "A high-performance MIMO OFDM wireless LAN," *IEEE Communications Magazine,* vol.43, no.2, pp.101-109, Feb. 2005.

[7] D. P. McNamara, M. A. Beach, P. N. Fletcher and P. Karlsson, "Initial investigation of multiple-input multiple-output (MIMO) channels in indoor environments," *Symposium on Communications and Vehicular Technology, 2000. SCVT-200*, pp.139-143, 2000.

[8] Hajime Suzuki, Thi Van Anh Tran, and Iain B. Collings, "Characteristics of MIMO-OFDM Channels in Indoor Environments," *EURASIP Journal on Wireless Communications and Networking*, vol. 2007, Article ID 19728, 9 pages, 2007.

[9] Hun Seok Kim, Weijun Zhu, Jatin Bhatia, Karim Mohammed, Anish Shah, and Babak Daneshrad, "A Practical, Hardware Friendly MMSE Detector for MIMO-OFDM-Based Systems," *EURASIP Journal on Advances in Signal Processing,* vol. 2008, 14 pages, 2008.

[10] T. M. Schmidl, D. C. Cox,"Robust frequency and timing synchronization for OFDM," *Communications, IEEE Transactions on* , vol.45, no.12, pp.1613-1621, Dec 1997.

[11] N. Maeda, T. Kataoka, H. Kawai, K. Higuchi, J. Kawamoto and M. Sawahashi, "Experiments on real-time 1-Gbps packet transmission using antenna-independent AMC in MIMO-OFDM broadband packet radio access," *IEEE Vehicular Technology Conference, 2005*. VTC-2005-Fall. 2005 IEEE 62nd , vol.3, pp. 1628-1632, 25-28 Sept., 2005.

[12] A. van Zelst and T. C. W. Schenk, "Implementation of a MIMO OFDM-based wireless LAN system," *IEEE transactions on Signal Processing*, vol.52, no.2, pp. 483-494, Feb. 2004.

[13] S. Haene, D. Perels and A. Burg, "A Real-Time 4-Stream MIMO-OFDM Transceiver: System Design, FPGA Implementation, and Characterization," *IEEE Journal on Selected Areas in Communications*, vol.26, no.6, pp.877-889, August 2008.

[14] W. Zhu, B. Daneshrad, J. Bhatia, J. Chen, H.-S. Kim, K. Mohammed, O. Nasr, S. Sasi, A. Shah, and M. Tsai, "A real time MIMO OFDM testbed for cognitive radio & networking research," in WiNTECH '06, New York, NY,USA: ACM Press, 2006, pp. 115–116.